Research Article

Neha Rana, A. Najitha Banu*, Rudradeb Sarkar, Ankush M. Raut, Amine Assouguem*, Ghadeer M. Albadrani, Muath Q. Al-Ghadi, Amany A. Sayed, and Mohamed M. Abdel-Daim

Green synthesis of sea buckthorn-mediated ZnO nanoparticles: Biological applications and acute nanotoxicity studies

https://doi.org/10.1515/gps-2025-0004
received January 05, 2025; accepted July 16, 2025

Abstract: Plant-based nanoparticle synthesis is the primary focus of modern nanotechnology to reduce the toxicity risk and ensure environmental safety. Zinc oxide nanoparticles (ZnO-NPs) were synthesized in the present investigation using an aqueous extract composed of sea buckthorn berries, adopting a biogenic approach. The green synthesized ZnO nanoparticles (NPs) exhibited a significant absorption peak near 370 nm in the UV–Vis spectrum. Fourier transform infrared study revealed the functional moieties responsible for the stability and capping of ZnO-NPs. The average particle size of the synthesized ZnO-NPs was 52.6 ± 12.51 nm, and their morphologies ranged from spherical to irregular, as indicated by the field emission scanning electron microscopy analysis. X-Ray diffraction study revealed the hexagonal wurtzite-structured NPs with an average particle size of 19.2 nm. The zeta potential of −20 mV indicated the colloidal stability of synthesized NPs. The biogenic ZnO-NPs were assessed for their antioxidant, antidiabetic, and anti-lipid peroxidation potential, where ZnO-NPs have shown better activity than the berry extract. Notably, the antimicrobial efficacy of the synthesized ZnO-NPs was observed against Gram-positive bacteria *Staphylococcus aureus* MTCC 3160 and Gram-negative bacteria *Escherichia coli* MTCC 1698, with the zone of inhibition observed as 18 ± 0.23 mm and 39 ± 1.24 mm, respectively. The minimum inhibitory concentration for S. *aureus* and *E. coli* was reported to be 0.5 and 1.0 mg·mL^{-1}, respectively. The LC_{50} for Daphnia was reported to be 16.09 mg·mL^{-1}, confirming the safety of the green-synthesized ZnO-NPs.

Keywords: green synthesis, Sea buckthorn, characterization, antioxidant, anti-diabetic, anti-lipid peroxidant, antibacterial, nanotoxicity

*** Corresponding author: A. Najitha Banu,** Department of Zoology, School of Bioengineering and Biosciences, Lovely Professional University, Phagwara, Punjab, India, e-mail: najirila2010@gmail.com
*** Corresponding author: Amine Assouguem,** Ethnopharmacology and Pharmacognosy Team, Faculty of Sciences and Technology, Errachidia, Moulay Ismaïl University, Meknes, Morocco, e-mail: assougam@gmail.com
Neha Rana, Rudradeb Sarkar: Department of Zoology, School of Bioengineering and Biosciences, Lovely Professional University, Phagwara, Punjab, India
Ankush M. Raut: Department of Entomology, School of Agriculture, Lovely Professional University, Phagwara, Punjab, India
Ghadeer M. Albadrani: Department of Biology, College of Science, Princess Nourah bint Abdulrahman University, 84428, Riyadh, 11671, Saudi Arabia
Muath Q. Al-Ghadi: Department of Zoology, College of Science, King Saud University, P.O. Box 2455, Riyadh, 11451, Saudi Arabia
Amany A. Sayed: Zoology Department, Faculty of Science, Cairo University, Giza, 12613, Egypt
Mohamed M. Abdel-Daim: Department of Pharmaceutical Sciences, Pharmacy Program, Batterjee Medical College, P.O. Box 6231, Jeddah, 21442, Saudi Arabia; Pharmacology Department, Faculty of Veterinary Medicine, Suez Canal University, Ismailia, 41522, Egypt

1 Introduction

Phytonanotechnology harnesses bioactive compounds like alkaloids, flavonoids, polyphenols, proteins, and enzymes from plants. These phytochemicals act as reducing, capping, and stabilization of nanoparticles (NPs). Plants have a rich repository of phytoconstituents that are frequently used in the synthesis of various metal-based NPs. The secondary metabolites present in the plants contain carbonyl, hydroxy, and amine functional groups that reduce them into nanoscale particles in reaction with metal ions [1]. Apart from bioreduction, the phytoconstituents act as stabilizing and capping agents, increasing the synthesized nanoparticles' biocompatibility [2,3]. Researchers have increasingly adopted green synthesis approaches utilizing various plant parts to minimize the environmental impact and health issues associated with traditional physical and chemical synthesis methods [4]. Conventional physicochemical techniques employed in the fabrication of

nanostructures involve the exploitation of toxic materials and specific reaction conditions (high temperature and pressure) [5]. These techniques are environmentally hazardous, energy-intensive, and threaten the ecosystem. Consequently, the use of plants has embarked on the facile, cost-effective, biocompatible, scalable, and eco-friendly synthesis of NPs, leading to phyto nanotechnology [6].

Nanotechnology encompasses creating and utilizing materials at the nanoscale (ranging from 1 to 100 nm), where particles exhibit unique properties owing to their large surface area-to-volume ratio [7,8]. The unique characteristics of ZnO-NPs, such as a high exciton binding energy and a wide bandwidth, have attracted significant attention in recent studies [9]. ZnO-NPs have exceptional semiconductor characteristics due to their wide bandgap (3.37 eV) and significant exciton binding energy (60 eV). These features confer catalytic activities, photonic capabilities, UV filtration, anti-inflammatory effects, and wound-healing powers. Consequently, ZnO-NPs find applications in diverse sectors such as electronics, optics, cosmetics (e.g., sunscreen lotions), medicine, biosensing, and agronomy. The synthesis of nanomaterials offers an innovative base in the biomedical domain with diverse applications. ZnO-NPs possess vast potential in tremendous biological applications, including antioxidant, antimicrobial, antifungal, anti-inflammatory, anti-diabetic, wound-healing, drug delivery, gene delivery, biosensing, and biolabeling [10].

FDA approval of the U.S. Food and Drug Authority underscores the biocompatible nature of ZnO-NPs [11]. Zinc is a trace element that is critical to the synthesis of nucleic acids, proteins, and a variety of enzymatic reactions. In biological systems, Zn^{2+} is a key cofactor in numerous enzymes that are essential for cellular processes. ZnO is known to play a significant role in the individual defense system [12]. Strikingly, laboratory and animal-based experiments showed that nanosized ZnO particles exhibited minimal toxicity toward healthy cells. ZnO in nanoform improved the osteoblast function and did not cause any carcinogenicity, cytotoxicity, genotoxicity as well or toxicity in the reproductive potential of humans [13]. Consequently, the use of ZnO-NPs is considered non-toxic to healthy cells but sufficiently effective in inducing apoptosis in cancerous cells [14]. The studies indicate that biologically synthesized ZnO-NPs exhibit stronger antibacterial effects than chemically synthesized counterparts, even at low concentrations, against Gram-positive and Gram-negative bacteria [15]. Multitudinous plant-mediated syntheses of ZnO-NPs have been documented in the literature; however, initiatives involving medicinal plants have been scarce. As a result, a medicinally significant plant is necessary for the synthesis of NPs capable of encapsulating bioactive compounds with therapeutic properties [16–18]. In this light, Sea buckthorn, SBT *(Hippophae rhamnoides* L.), is a shrub indigenous to Asia and Europe, renowned for its orange berries. Sea buckthorn is an important plant in traditional medicine and scientific research due to its abundance of minerals, bioactive compounds like flavonoids (quercetin, kaempferol, and isorhamnetin), carotenoids (β-Carotene), and a repertoire of vitamins (C-, E-, and B-complexes) [19]. Additionally, this plant is rich in essential fatty acids such as omega-3,6,7 and 9, along with important minerals like calcium, magnesium, potassium, and iron [20–22]. Due to the abundance of phytochemicals, SBT has immunomodulating and antioxidative properties, antiatherogenic and cardioprotective effects, antibacterial and antiviral effects, healing effects on acute and chronic wounds, antiradiation properties, anti-inflammatory effects, antidiabetic properties, anticarcinogenic effects, as well as hepatoprotective and dermatological effects [23,24]. Due to this rationale, sea buckthorn leaves and berries are extensively utilized for nutraceutical and therapeutic applications. Notwithstanding its remarkable phytochemical composition, there are just a few documented instances of *H. rhamnoides* being utilized in nanoparticle synthesis, predominantly with flower-shaped ZnO-NPs and dye degradation applications [25].

This report represents the first documentation of the green synthesis of spherical to irregular ZnO-NPs utilizing *H. rhamnoides* L. berry extract and zinc sulfate as a precursor, to investigate their antioxidant, antidiabetic, anti-lipid peroxidation, antimicrobial efficacy, and acute nanotoxicity assessed through *Daphnia* sp. This study identifies a gap in biomedical research concerning medicinal plant-derived ZnO-NPs and proposes a unique, safe, and biologically effective nanomaterial for potential therapeutic uses.

2 Materials and methods

2.1 Chemicals and reagents

All the chemicals used in the current investigation were of analytical grade. Zinc sulfate hexahydrate (≥99% purity), ascorbic acid (≥99%), 2,2-diphenyl-1-picrylhydrazyl (DPPH, ≥95%), thiobarbituric acid (TBA) (≥98%), potassium chloride (≥99%), 2,2-diphenyl-1-picrylhydrazyl (DPPH, ≥95%), TBA (≥98%), potassium chloride (≥99%), sodium hydroxide (≥97%), sodium dodecyl sulfate (SDS, ≥99%),

acetic acid (≥99.7%), streptomycin (≥98%), butanol (≥99%), α-amylase (≥97%), starch (soluble, ≥99%), ferrous sulfate (≥99%), Mueller Hinton agar, and Luria broth were procured from Loba Chemie (Mumbai, India).

2.2 Preparation of plant extract

The berries of sea buckthorn, SBT (*Hippophae rhamnoides*), were sourced from Ladakh, India. A taxonomist from CSIR, IHBT Palampur, verified the plant with voucher number PLP 24625. The berries were washed to remove the impurities, dried, and crushed into a fine powder. In distilled water, 2% aqueous plant extract was prepared by boiling the mixture for 20 min at 80–90°C [26]. Whatman No. 1 filter paper was employed to filter the plant fraction. The filtrate obtained was utilized as a reductant and stabilizing agent for the synthesis of NPs.

2.3 Biogenic synthesis of ZnO-NPs

ZnO-Nps were synthesized following a protocol that had been previously reported, with minor modifications [27]. Briefly, the fresh SBT aqueous extract was gradually added to the 50 mM solution of $ZnSO_4$ in a 1:1 ratio. The starting pH of the reaction mixture was recorded to be 4, and then 1N NaOH was added dropwise to keep the pH at 8. The reaction mixture was stirred using a magnetic stirrer for 2 h for the complete reduction of $ZnSO_4$ till the formation of white precipitates. Further, the process of decantation was followed, and the resulting material was collected and repeatedly washed with distilled water. Next, the material was oven-dried, and creamy white powder of ZnO-NPs was collected [28,29]. The resulting powder was stored in a desiccator for characterization and further experimentation (Figures 1 and 2).

2.4 Characterization of ZnO-NPs

The synthesized AgNPs were characterized by using different physicochemical techniques. The preliminary verification of green AgNPs was done using a UV–Vis spectroscope (Lasany Model No. LI-2800). Fourier transform infrared (FTIR) (Perkin Elmer Spectrum 2) analysis was performed to show the presence of phytochemicals accountable for the stabilization and capping of ZnO-NPs. The morphology and size of fabricated ZnO-NPs were examined with Field emission scanning electron microscopy (FE-SEM) (JEOL JSM-7610F). EDAX was used to detect

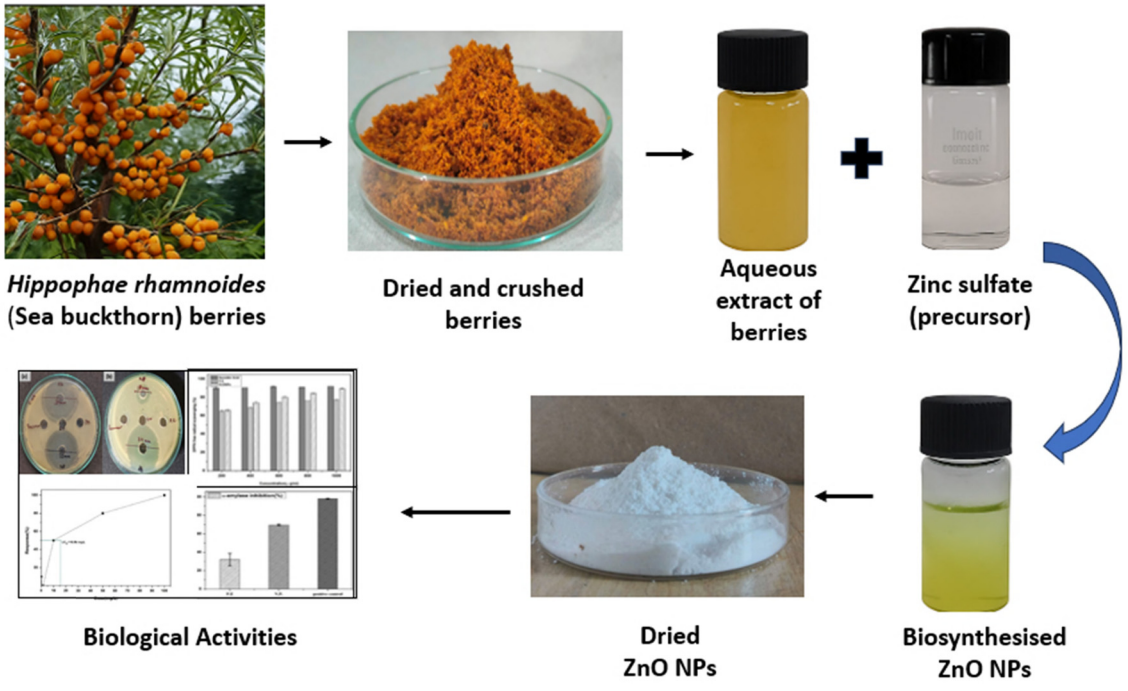

Figure 1: Graphical abstract illustrating the phytofabrication of ZnO-NPs mediated by *Hippophae rhamnoides* (Sea buckthorn) berry extract. The process includes the preparation of aqueous extract, nanoparticle synthesis with zinc sulfate, drying, and evaluation of biological properties.

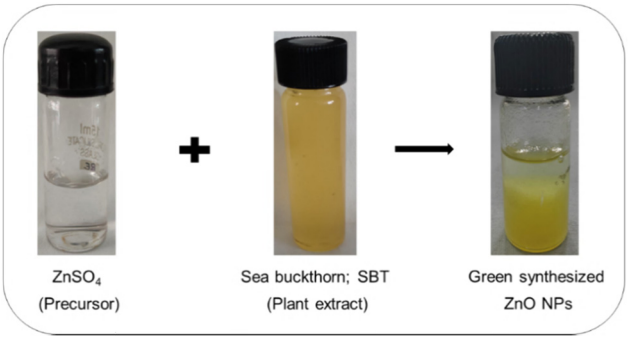

Figure 2: Pictorial representation showing color change (yellowish-white) as the initial visual confirmation of ZnO nanoparticle synthesis during green synthesis.

the presence of elemental zinc in phytofabricated ZnO-NPs. X-ray diffraction (XRD) (Bruker D8 Advance) examination was conducted to ascertain the crystalline structure of the synthesized NPs. Additionally, zeta potential (Malvern Zetasizer Nano ZS90) analysis was carried out to assess the stability and surface charge of the suspended NPs.

2.5 Antioxidant activity

The antioxidant potential of bio-fabricated ZnO-NPs was evaluated using the 2,2-diphenylpicrylhydrazyl (DPPH) assay [30]. A fresh stock solution of DPPH was formulated by mixing 5.5 mg in 25 mL of methanol. Methanol was used to dilute the stock solution to obtain an O.D. (optical density) between 0.8 and 1.0. Five varied concentrations (1,000, 800, 600, 400,200 $\mu g \cdot mL^{-1}$) of P.E., AgNPs, and ascorbic acid (as standard) were used as test samples. Further, the test samples (P.E., AgNPs, and ascorbic acid) were mixed with 1 mL of DPPH solution. For half an hour, the resultant mixture was incubated in the dark. The absorbance was taken at a wavelength of 517 nm using a UV–Visible spectrophotometer. The DPPH mixture was used as a blank, and Methanol was used as a control. The experiment was carried out in triplicate. The % inhibition of DPPH free radicals was computed using the absorbance of the control (A_c) and test (A_t) by applying the following Eq. 1:

$$\% \text{ Inhibition} = (A_c) - (A_t)/(A_c) \times 100 \quad (1)$$

2.6 Anti-lipid peroxidation potential

To quantify the *in vitro* anti-lipid peroxidation efficacy of the biosynthesized AgNPs and P.E., a modified Thio Barbituric Acid Assay (TBARS) was used [31]. Briefly, Malondialdehyde, a byproduct of lipid peroxidation (LPO), interacts with two molecules of TBA, resulting in the formation of a pinkish-red chromogen with a maximum absorbance at λ_{max} = 532 nm. Egg yolk, being a lipid-rich medium, was utilized in the experiment. For the experimentation, the egg yolk homogenate was initially prepared by mixing egg yolk (10% v/v) with potassium chloride (KCl) (1.15% w/v). The egg yolk was ultrasonicated for 5 min for proper mixing. Next, 0.5 mL of plant extract and ZnO-NPs were added to 0.5 mL of yolk homogenate. Subsequently, 50 mL of Ferrous sulfate (0.07 mM) was combined, and the mixture was left to incubate for 30 min at 27–30°C. After incubation, 1.5 mL of TBA solution (made with 1.1% SDS solution) and 1.5 mL of acetic acid were added to the test tubes. After vortexing for 1 min, the mixture was heated to 95°C for 1 h in a water bath. Following cooling, 5.0 mL of butanol was mixed into each tube. After 10 min of centrifugation at 3,000 rpm, a maximum absorbance of the upper butanol layer was observed at 532 nm. The % inhibition of LPO was determined using Eq. 1.

2.7 Anti-diabetic potential

The SBT aqueous extract and fabricated Zn ONPs have been studied for anti-diabetic effects using the α-amylase inhibition assay by following the methodology of Majeed et al. with slight modifications [32]. First of all, 100 µL of varied concentrations of AgNPs (500, 400, 300, 200, and 100 $\mu g \cdot mL^{-1}$) was added to 250 µL of α-amylase and incubated for 30 min at 25–27°C. The mixture was left to incubate for 10 min at room temperature following the addition of 1% starch solution. Subsequently, 250 µL of $FeSO_4$ was added, and the mixture was allowed to stand at room temperature for 5 min. The solution was incubated in a water bath at 85°C for 10 min, and its optical density was measured at 540 nm. Eq. 1 was used to determine the percentage inhibition of α-amylase. The entire experiment was performed in triplicate.

2.8 Minimum inhibitory concentration (MIC)

To determine the MIC of the synthesized material against *E. coli* (MTCC 1698) and *S. aureus (*MTCC 3160), a 96-titre plate method containing different concentrations of the material was followed. In this experiment, the 24-h-grown bacterial cultures were double-diluted with Mueller-Hinton broth. 100 µL of bacterial culture was added with 100 µL of different concentrations of ZnO-NPs (1, 0.75, 0.5, 0.25, and 0.125 $mg \cdot mL^{-1}$) in the wells. Positive (antibiotic) and negative

(DW) controls were also poured into the wells containing bacterial cultures. The 96-well titer plate was incubated at 37°C for 24 h. The next day, the absorbance of the bacterial culture was checked using a plate reader at 595 nm, and the calculation of % inhibition was done using the Eq. 2:

$$\% \text{ inhibition} = \text{OD of bacterial culture} - \text{OD of test sample/OD of bacterial culture} \times 100 \quad (2)$$

2.9 Minimum bactericidal concentration (MBC)

The MBC of ZnO-NPs was performed after calculating its MIC value using the spot method. Bacterial cultures containing two high and two lower concentrations of ZnO-NPs, along with the MIC value, were spotted on the MHA plate. The plates were left to incubate at 37°C overnight. The growth of bacteria was checked on the plate after 24 h.

2.10 Antimicrobial efficacy

The antibacterial potential of P.E. and SBT-ZnO-NPs was estimated by a well diffusion method against *E. coli* and *S. aureus*. The bacterial cultures were revived on Luria Bertani Broth at 37°C for 24 h. After sterilizing the MHA media in an autoclave, it was poured into sterilized Petri dishes and allowed to solidify under a laminar flow hood [33]. Subsequently, the bacterial culture of 100 µL was evenly spread onto MHA plates. A sterilized borer was used to make wells in the agar plates. Then, wells were loaded with 100 µL of (1.0 mg·mL^{-1} for *E. coli* and 0.5 mg·mL^{-1} for *S. aureus*) streptomycin (positive control), distilled water (negative control), $ZnSO_4$ (precursor), ZnO-NPs, and plant extract (P.E.). The experiment was performed in triplicate. The zone of inhibition was determined in mm by measuring the diameter of the clear area around the wells.

2.11 Nanotoxicity studies

The standard OECD guidelines 202 were followed to study the acute toxicity in *Daphnia* [34]. *Daphnia* was grown in freshwater under typical environmental conditions, maintaining a 16:8 light-dark cycle at a temperature of 22 ± 2°C. The culture was sustained in the laboratory for 6 months, utilizing pond water as a food source [30]. In this investigation, *Daphnia* neonates (under 24 h old) were chosen from a stable culture to function as test organisms for the acute toxicity experiments. The 48-h acute toxicity (LC_{50}) assessment was performed on neonates subjected to different concentrations of ZnO-NPs (0.1, 0.5, 1.0, 5.0, 10.0, and 100 mg·L^{-1}), with distilled water serving as the negative control. A total of 10 neonates (≤24 h old) were utilized, and the experiment was conducted three times. Each group received 30 mL of the test material in 50 mL containers. The number of immobile *Daphnia* was recorded 48 h after treatment. According to OECD criteria, *Daphnia* were considered dead if they remained motionless for 15 s following gentle agitation. Probit analysis was employed to get the LC_{50} value and its 95% confidence intervals.

3 Results

3.1 UV–Vis spectroscopy

The UV–vis spectroscopy technique is useful for the preliminary assessment of nanoparticle synthesis. The UV–Vis absorption spectrum of ZnO-NPs has a peak around 370 nm,

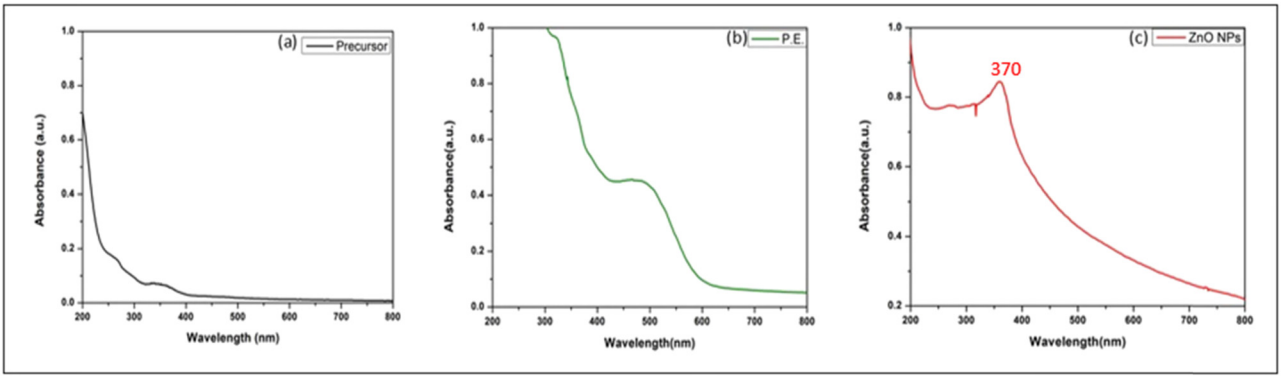

Figure 3: UV–Vis absorption spectra of (a) Zinc sulfate (precursor), (b) P.E. (SBT), and (c) biogenic ZnO-NPs.

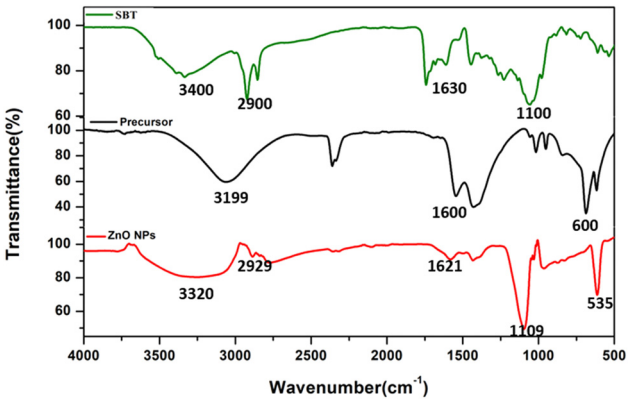

Figure 4: FT-IR Profile of P.E., precursor, and green synthesized Zn ONPs with a spectral range of 500–4,000 cm^{-1}.

indicating the successful production of ZnO-NPs from SBT extract (Figure 3c). This corresponds to a band gap energy of approximately 3.37 eV, facilitating electron excitation.

3.2 FT-IR analysis

FT-IR Spectra (500–4,000 cm^{-1}) were employed to ascertain the functional groups implicated in the production of ZnO-NPs from the aqueous SBT extract, as illustrated in Figure 4. The FTIR spectra of the Hippophae rhamnoides extract (SBT), zinc sulfate precursor, and synthesized ZnO nanoparticles (ZnO-NPs) were examined to elucidate the functional groups implicated in nanoparticle synthesis and stabilization. The SBT extract exhibited distinct peaks at around 3,400 cm^{-1} (O–H stretching of alcohols and phenols), 2,920 cm^{-1} (C–H stretching), 1,600–1,650 cm^{-1} (C═O stretching of carbonyl groups), and 1,000–1,200 cm^{-1} (C–O stretching) [35]. The precursor exhibited extensive O–H stretching and bending vibrations, affirming the presence of absorbed water molecules. The precursor spectrum has a broad band at 3,400 cm^{-1} and a peak at 1,600 cm^{-1}, indicative of water molecules, while pronounced bands between 1,000 and 1,100 cm^{-1} result from S═O stretching of sulfate ions. A minor signal at 600 cm^{-1} is ascribed to O–S–O bending vibrations of sulfate moieties. The ZnO-NP spectra have a large peak at approximately 3,400 cm^{-1}, indicative of surface-bound hydroxyl groups, whereas peaks around 2,900 and 1,600 cm^{-1} are associated with remaining organic molecules, implying partial capping by phytochemicals [36]. These available functional groups in the SBT (P.E.) provided electrons, which reduced zinc ions (Zn^{2+}) to Zn^{+} and finally reduced to ZnO-NPs. The energy band ascribed to 1,600–1,700 cm^{-1} shows carbonyl bonds, typically from proteins or organic acids that serve as stabilizers [37]. Peaks detected between 1,000 and 1,100 cm^{-1} further corroborate the existence of C–O–C bonds originating from plant-derived proteins. The FTIR spectra showed a distinct band at 546 cm^{-1}, indicating Zn–O (zinc-oxygen) vibrations, and the strong signal verifies the synthesis of ZnO-NPs [38]. The existence of intermediate peaks indicates that phytochemicals from the plant extract played a role in the reduction, capping, and stabilization of the NPs.

3.3 FE-SEM

FE-SEM was used to analyze the size and morphology of the biosynthesized ZnO-NPs (Figure 5). The average size of the

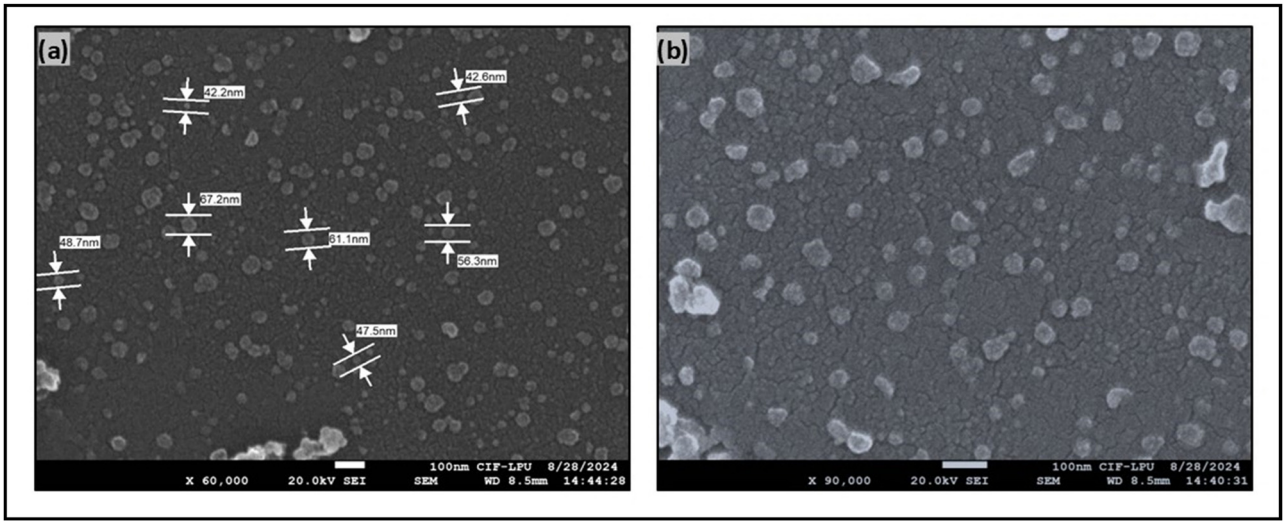

Figure 5: Representative images from FE-SEM analysis of biogenic ZnO-NPs (a) at 75,000× magnification, (b) at 1,00,000× magnification.

synthesized ZnO-NPs was reported to be in the range of 52.6 ± 12.51 nm, which was found to be comparable to the previously green-synthesized ZnO-NPs [5].

3.4 Energy dispersive X-ray spectroscopy (EDX)

EDX is an advanced approach to accessing the elemental composition of the material, providing comprehensive information about the types and quantities of elements present. The EDAX spectra revealed zinc peaks at 3.0 and 3.1 keV, validating the chemical composition of the biogenic ZnO-NPs (Figure 6). The EDX spectrum exhibits a pronounced signal for Zn, while C, O, and Ca display diminished signals. The weak signals are due to macromolecules, including enzymes, proteins, and carbohydrates present in plant cell walls, which produce X-rays during examination.

3.5 XRD

The ZnO-NPs that were synthesized showed diffraction peaks at 2θ values of about 31.7°, 34.4°, 36.2°, 47.5°, 56.6°, 62.9°, and 68.0°. These peaks corresponded to the (100), (002), (101), (102), (110), and (113) planes, in that order (Figure 7). The hexagonal wurtzite structure of ZnO, which can be seen on JCPDS card No. 36-1451, aligns well with these reflections [39]. Additional

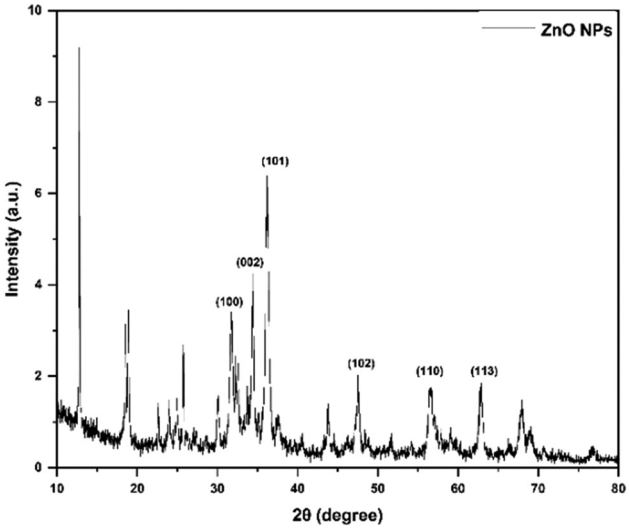

Figure 7: XRD pattern of ZnO-NPs prepared by green synthesis.

peaks were observed at 12.9°, 26.6°, and 30.6° in addition to Bragg's peaks for the zinc nanocrystal. These supplementary peaks may be attributed to the biomolecules in the plant extract, implying that the bio-organic phase crystallizes on the surface of ZnO-NPs [40].

XRD measurement revealed an average crystalline size of approximately 19.2 nm for the synthesized ZnO-NPs, as determined by following Debye–Scherrer's equation.

$$D = 0.94\lambda/(\beta \cos \theta)$$

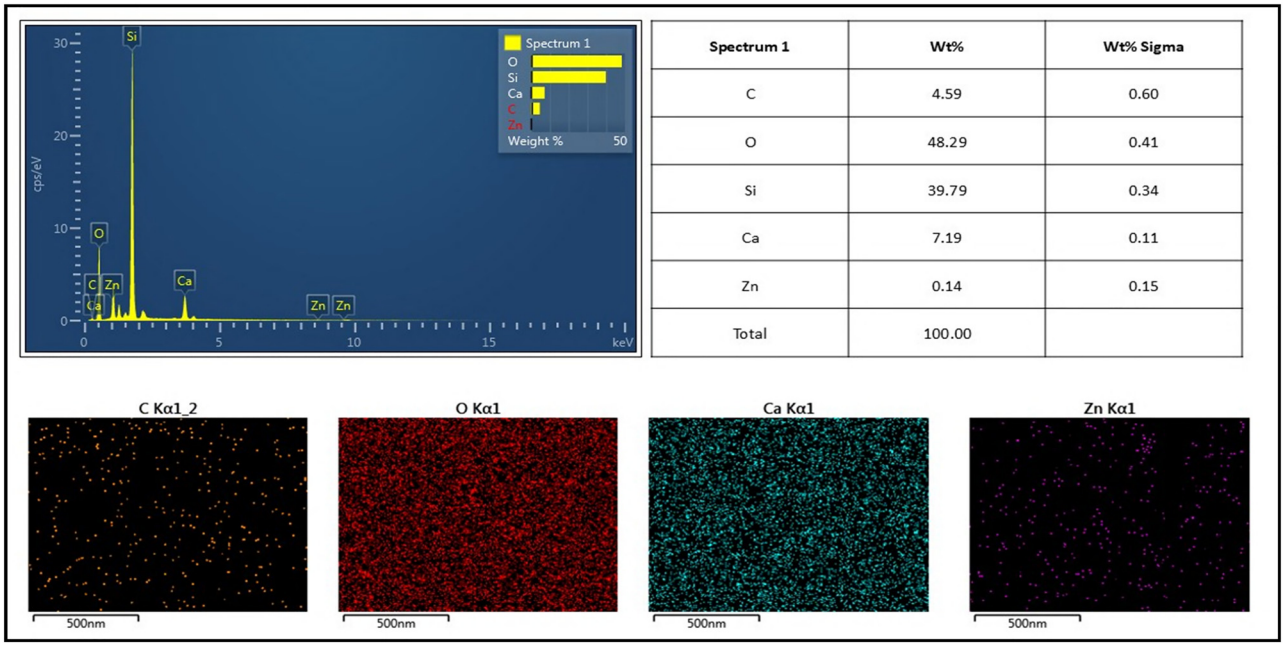

Spectrum 1	Wt%	Wt% Sigma
C	4.59	0.60
O	48.29	0.41
Si	39.79	0.34
Ca	7.19	0.11
Zn	0.14	0.15
Total	100.00	

Figure 6: EDX Analysis and elemental mapping of Zn-NPs; with EDX graph, molecular mapping of ZnO-NP powder along with an individual elemental map of carbon, oxygen, calcium, and zinc.

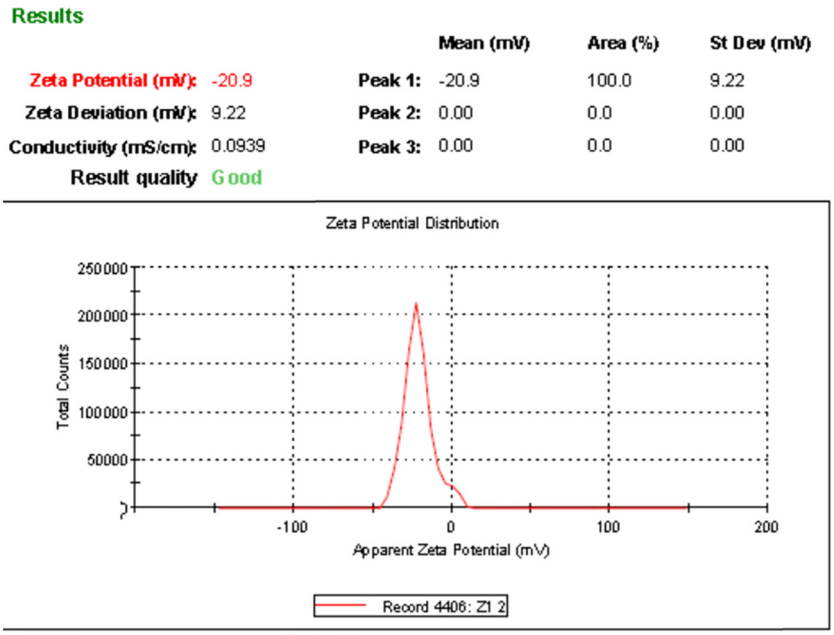

Figure 8: Zeta potential analysis of biosynthesized ZnO-NPs confirming surface charge and colloidal stability.

where D = crystallite size, 0.94 = Scherrer's constant, λ = X-ray wavelength (1.5406), θ = Bragg diffraction angle, β = full width at half-maximum.

The observed size disparity between FESEM and XRD measurements can be ascribed to XRD's information on the crystallite size, whereas FESEM shows the total particle size, which might include aggregates or polycrystalline structures developed by the coalescence of smaller grains [41].

3.6 Zeta potential

The synthesized ZnO-NPs demonstrated a zeta potential of −20.9 mV, signifying colloidal stability (Figure 8). A

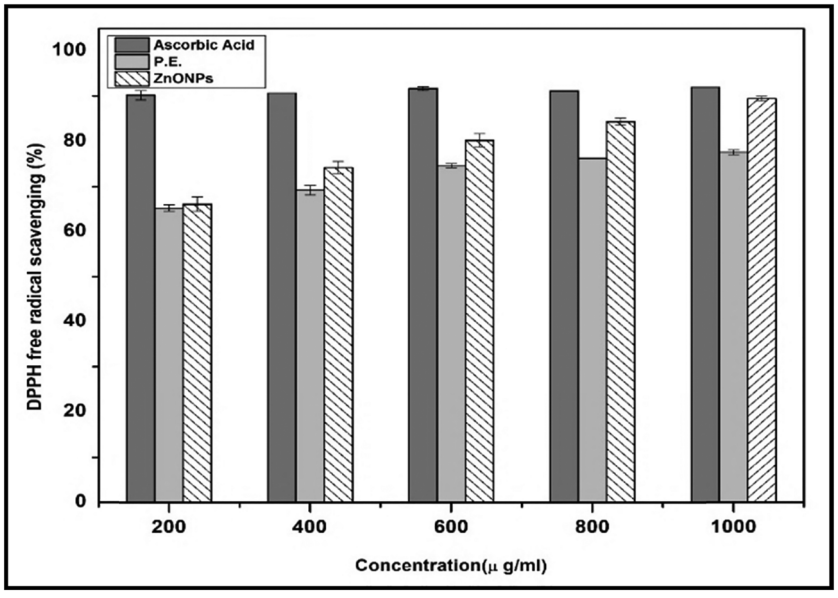

Figure 9: The DPPH free radical quenching activity was evaluated for different concentrations of ZnO-NPs, P.E., and ascorbic acid (standard). The results are presented as mean ± S.D. (n = 3).

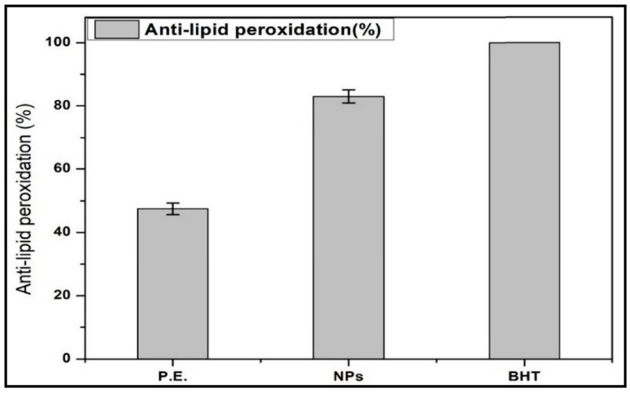

Figure 10: TBARS Assay representing LPO inhibition by ZnO-NPs, P.E, and BHT (standard).

singular, sharp peak validated a homogeneous particle distribution devoid of agglomeration.

3.7 *In vitro* antioxidant activity

The outcomes in Figure 6 showed that both SBT (P.E.) and ZnO-NPs demonstrated considerable antioxidant activity by scavenging free radicals, with efficacy increasing dose-dependently (Figure 9). ZnO-NPs exhibited better antioxidant potential than PE out of five concentrations (1,000, 800, 600, 400, 200 $\mu g \cdot mL^{-1}$).

3.8 LPO inhibition potential

The fabricated ZnO-NPs and SBT berries extract showed a potential to inhibit LPO in the egg homogenate using the TBARS assay. The ZnO-Nps depicted a better inhibition of 83.01 ± 2.09% compared to 47.47 ± 1.84% in the case of SBT (P.E.). The butylated hydroxytoluene used as a standard showed 100% inhibition (Figure 10).

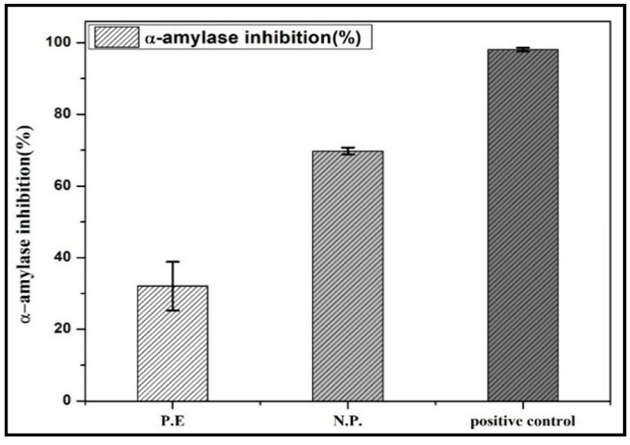

Figure 11: Anti-diabetic efficacy of SBT-synthesized ZnO-NPs, P.E. (SBT), and maltose (standard).

3.9 *In vitro* anti-diabetic activity

The effect of the *in vitro* anti-diabetic test was assessed using the enzyme α-amylase, which is important for the metabolism of carbohydrates. The ZnO-NPs showed the inhibition of α-amylase enzyme around 69.73 ± 1.11%, whereas the P.E. inhibited the enzyme up to 32.04 ± 6.80%. Maltose was utilized as a positive control and displayed 100% inhibition (Figure 11).

3.10 MIC

The MIC data (Table 1) for *E. coli* show that a concentration of 1.0 $mg \cdot mL^{-1}$ inhibited growth by 76.25 ± 3.02%. A growth inhibition of 77.81 ± 1.07% was reported at 0.75 $mg \cdot mL^{-1}$, with an insignificant difference between the two concentrations. Hence, 1.0 $mg \cdot mL^{-1}$ was chosen as the MIC for *E. coli* in this investigation. Regarding *S. aureus,* the MIC was calculated to be 0.5 $mg \cdot mL^{-1}$, where the highest growth inhibition % was reported to be 58.08 ± 2.54%.

3.11 MBC

Based on MIC studies, the values of MBC were selected. Two concentrations above and two concentrations below the MIC value were considered for the study of MBC. For *E. coli*, MBC was reported to be 1.0 $mg \cdot mL^{-1}$, and for *S. aureus,* it was found to be 0.5 $mg \cdot mL^{-1}$ (Figure 12).

3.12 Antimicrobial efficacy

The antibacterial effectivity of phytofabricated ZnO-NPs was evaluated using the well diffusion method. The NPs, plant

Table 1: Depiction of percentage growth inhibition of green-synthesized ZnO-Nps against *E. coli* and *S. aureus*

Concentration ($mg \cdot mL^{-1}$)	Growth inhibition (%)	
	E. coli	*S. aureus*
1.0	76.25 ± 3.02	25.54 ± 3.79
0.75	77.81 ± 1.07	50.49 ± 1.85
0.5	70.48 ± 1.20	58.08 ± 2.54
0.25	46.78 ± 2.82	56.68 ± 2.41
0.125	46.08 ± 1.56	35.92 ± 7.68

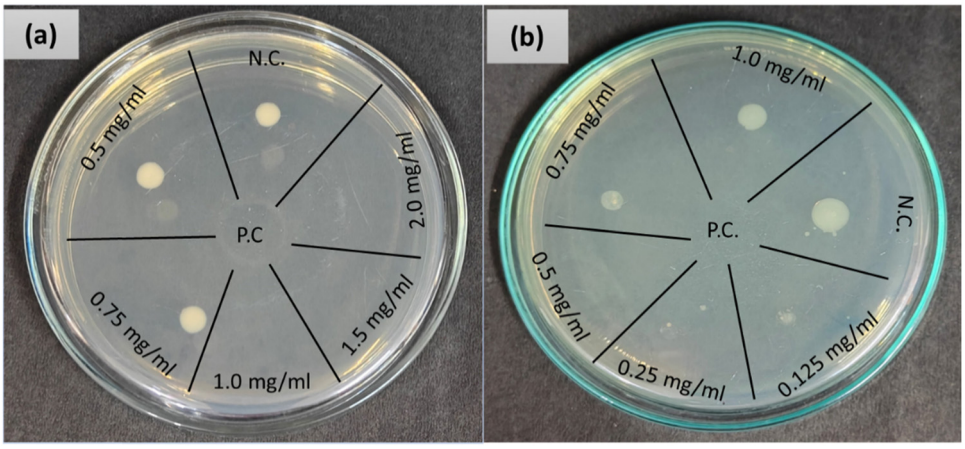

Figure 12: MBC results across different concentrations of ZnO-NPs: (a) *E. coli* and (b) *S. aureus*. NC, Negative control; P.C., positive control.

extract, and $ZnSO_4$ were examined for their antibacterial potential against *E. coli* and *S. aureus*. The zone of inhibition for *E. coli* (MTCC 1698) and *S. aureus* (MTCC 3160) was recorded to be 33 ± 1.24 mm and 18 ± 0.23 mm, as compared to standard antibiotic streptomycin, which was reported to be 39 ± 1.12 mm and 34 ± 1.67 mm, respectively. On the contrary, the aqueous P.E. of SBT did not show any inhibition against the tested bacteria. Distilled water was utilized as a negative control and exhibited no zone of inhibition (Figure 13).

3.13 Acute nanotoxicity studies

The ZnO-NPs with varying concentrations from 0.1–100 $mg{\cdot}L^{-1}$ showed an LC_{50} value of 16.09 $mg{\cdot}L^{-1}$ after the exposure of 48 h, as calculated through prohibit analysis (Figure 14).

Hence, a concentration below 16.09 $mg{\cdot}L^{-1}$ is considered safe for *Daphnia*. Table 2 depicts the LC_{50} value of previously fabricated ZnO-NPs against *Daphnia*.

4 Discussion

Plants have bioactive pharmacological chemicals that can notably improve the pharmacological activity of NPs by acting as reducing, stabilizing, and capping molecules. This approach promotes green technology by minimizing the raw materials required for the synthesis of NPs, which typically depend on chemicals, solvents, and energy consumption. Plant-based methods for green synthesis reduce the reliance on traditional physicochemical materials, providing a more sustainable and environmentally friendly

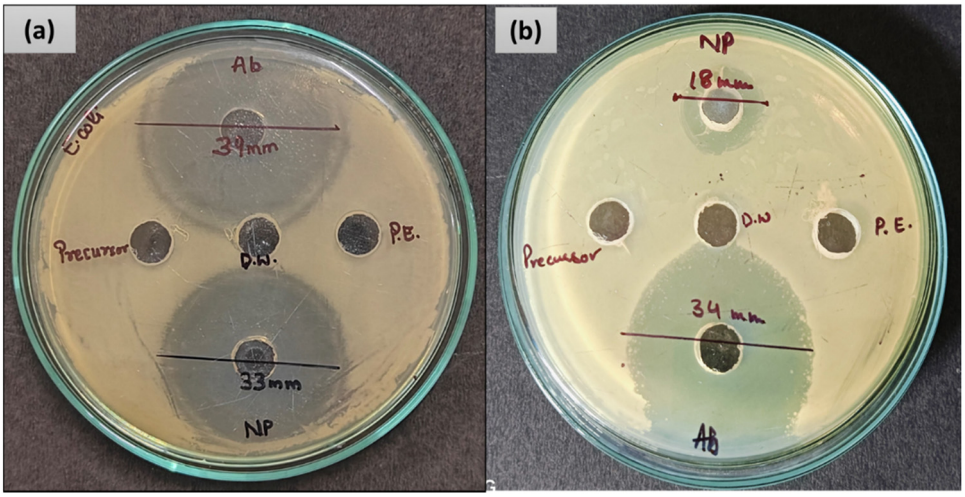

Figure 13: The antimicrobial potential of ZnO-NPs synthesized from SBT was evaluated against (a) *E. coli* and (b) *S. aureus*. The data are presented as mean ± SD for $n = 3$.

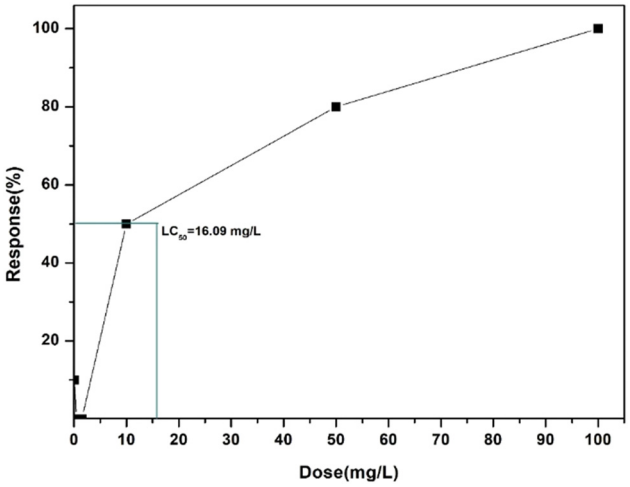

Figure 14: LC_{50} value of green synthesized ZnO-NPs after the exposure of 48 hours, calculated through prohibit analysis.

Table 2: ZnO-NPs synthesized using different methods and their LC_{50} values

S. no.	Zn ONPs	Size	LC_{50}	References
1.	Chemical precipitation method	80–100 nm	1.32 mg·L^{-1}	[42]
2.	Chemical synthesis	40 nm 60 nm	2.93 mg·L^{-1} 3.24 mg·L^{-1}	[43]
3.	Not available	Not available	0.3 mg·L^{-1}	[44]
4.	Chemical synthesis	20 nm	1.511 mg·L^{-1}	[45]
5.	SBT synthesized	52.67 nm	16.09 mg·L^{-1}	Present study

The present study depicts higher LC_{50} values, ensuring the safety of the tested NPs against the *Daphnia* culture.

alternative [45]. Additionally, the single-step biosynthetic process of plant-mediated nanoparticle synthesis is considered simple, safe for therapeutic applications, cost-effective, energy-efficient, and environmentally benign [46].

The current study focuses on the phytofabrication of ZnO-NPs from an aqueous extract of Sea buckthorn utilizing zinc sulfate as precursor salt. UV–visible spectra, FTIR, FE-SEM, and EDS were also used to characterize ZnO-NPs, and the results further verified the nanoscale size and shape of the fabricated NPs. The surface plasmon resonance of SBT-mediated ZnO-NPs was observed around 370 nm and found to be consistent with previous findings [11,47]. SBT aqueous extract was also subjected to UV–Vis spectroscopy revealed a peak at the range of 450 nm is indicative of phenolic acids and flavonols [48]. XRD examination validated the crystalline structure of the ZnO-NPs, with additional peaks indicating the presence of phytochemicals, suggesting that they are involved in stabilizing or coating the NPs during green synthesis. Similar peaks have been reported by many researchers [40,49]. A Zeta potential of −20.9 mV further substantiates excellent colloidal stability, inhibiting aggregation and enabling efficient dispersion [50].

In the present study, SBT-synthesized ZnO-NPs functioned as better antioxidants as compared to SBT berry extract, and the results align with prior findings [51]. NPs possess a larger surface area to volume, enhancing the number of active sites for reactions and facilitating improved interactions with free radicals compared to plant extracts. Additionally, there is a synergistic effect of NP surface properties and attached phytochemicals from plants, which aids in an enhanced antioxidant performance of green-synthesized ZnO-NPs. The tendency of antioxidants to donate hydrogen atoms or electrons makes them ideal for neutralizing DPPH radicals. A yellowish or brownish solution with reduced absorbance is produced when these electron/hydrogen donor molecules react with the DPPH radical, which typically displays a deep violet [47].

LPO is a cell-damaging mechanism caused by free radicals or chemicals that target cellular membranes, lipoproteins, and other lipid-containing components. This mechanism frequently causes irreversible cell damage, making it a major contributor to cell death [52]. In this work, ZnO-NPs surpassed the plant extract in protecting the lipid-rich media (egg yolk) against peroxidation. NPs, by their size, effectively inhibit LPO through various chemical pathways, including the addition and recombination of radicals, electron transfer, and free radical scavenging during the propagation phase of LPO [53]. ZnO-NPs have more antioxidant activity than crude plant extracts, making them more effective as chain-breaking radical scavengers and retarding LPO effectively [54,55]. This improved capacity enables NPs to neutralize free radicals more effectively, adding to their greater efficiency in reducing oxidative damage.

The present study shows that the SBT-mediated ZnO-NPs and SBT (P.E) both have shown an inhibition towards the α-amylase enzyme. When compared, biogenic ZnO-NPs were proved to be superior in the suppression of α-amylase enzyme as compared to the SBT aqueous extract. The findings are in line with findings obtained by various studies, where the antidiabetic activity of ZnO-NPs is documented [56,57]. NPs are sufficiently small to infiltrate cells and interact safely with cytoplasmic and genomic molecules, making them better antidiabetic agents [58]. According to previous research, ZnO-NPs exhibit anti-diabetic potential by enhancing insulin secretion, improving glucose tolerance and insulin sensitivity, boosting glucose uptake in key tissues, and inhibiting both lipolysis and gluconeogenesis [59,60].

As a part of the present study, the SBT-mediated ZnO-NPs displayed significant antibacterial efficiency against *E. coli* and *S. aureus*. The MIC data indicate that the optimal concentration of ZnO-NPs against *E. coli* is 1.0 mg·mL^{-1} with a maximum rate of inhibition of 76.25 ± 3.02%, whereas against *S. aureus* is reported to be 0.5 mg·mL^{-1} with 58.08 ± 2.69% of maximal inhibition rate. The antimicrobial potential of plant-based ZnO-NPs is well-cited in numerous studies [38]. It is hypothesized that NPs may target microbial cell membranes, causing membrane potential damage and, eventually, bacterial cell death. NPs, after entering cells, affect DNA replication and other protein functions, exacerbating cellular damage and eventually causing bacterial cell death. Additionally, it produces reactive oxygen species, which causes oxidative stress, cellular damage, and, eventually, cell death [61,62]. The results of the antibacterial assay revealed that ZnO-NPs are more effective against *E. coli* as compared to *S. aureus.* This may be because of the reason that Gram-positive bacteria have a thicker and harder peptidoglycan coating in their cellular wall, which makes them less prone to absorb NPs [63].

NPs, after being utilized frequently, leach out into the ecosystem and end up in water bodies, creating potential dangers that lead to nanotoxicity [41]. *Daphnia*, being freshwater plankton, is used as a sensitive indicator to assess toxicity in water bodies [64]. *Daphnia* species are thought to be representative of freshwater ecosystems and are sensitive to environmental toxins; they are frequently utilized in ecotoxicological analysis [30]. In this exploration, the LC_{50} value for *Daphnia* was reported to be 16.09 mg·L^{-1}, which is higher than the prior studies, suggesting the lower toxicity of the non-biologically synthesized NPs utilized [41–43]. It is well established that the higher the LC_{50} value lower the toxicity of the material, implying that a higher concentration is needed to kill 50% of the test population [65]. In the present study, the higher LC_{50} value of the green-synthesized ZnO-NPs underscores their importance in terms of environmental safety. This emphasizes the need for green synthesis that replaces hazardous chemicals with plant-based capping and stabilizing agents. These natural substances not only minimize toxicity but also improve the biocompatibility of NPs, implying a more ecologically responsible approach to their synthesis. Hence, green technology offers safer alternatives to reduce threats to aquatic organisms while remaining effective in biomedical applications.

5 Conclusion

The study emphasizes the role of sea buckthorn as a potential reductant and stabilizing agent for the effective phytofabrication of ZnO-NPs. The present synthesis is environmentally benign, operating under sustainable conditions with minimal toxic byproducts, positioning it as a greener alternative to traditional methods. The synthesized NPs showed a distinct absorption at 370 nm, and FTIR highlighted the role of SBT phytochemicals in the reduction of NPs. The morphology of ZnO-Nps as studied through FESEM reveals a spherical to irregular shape with a mean size of 52.6 ± 12.51 nm. The results of XRD hinted at the hexagonal structure of the synthesized ZnO-NPs. The biogenic ZnO-NPs have a pronounced antioxidant, anti-lipid peroxidation, and antidiabetic potential. The *in vitro* antimicrobial assay results against bacteria *E. coli* and *S. aureus* establish the green-synthesized ZnO-NPs as effective antimicrobial agents. Nanotoxicity Studies performed on the aquatic model organism *Daphnia* exhibited no lethality at concentrations up to 16.09 mg·L^{-1}, making the SBT-mediated ZnO-NPs safe to the environment. Hence, the SBT fabricated ZnO-NPs demonstrate significant suitability for medical applications, providing both efficacy and environmental safety.

Acknowledgments: This study was supported by Princess Nourah bint Abdulrahman University Researchers Supporting Project number (PNURSP2025R30), Princess Nourah bint Abdulrahman University, Riyadh, Saudi Arabia. This research was funded by the Researchers Supporting Project number (RSPD2025R811), King Saud University, Riyadh, Saudi Arabia.

Funding information: This study was supported by Princess Nourah bint Abdulrahman University Researchers Supporting Project number (PNURSP2025R30), Princess Nourah bint Abdulrahman University, Riyadh, Saudi Arabia. This research was funded by the Researchers Supporting Project number (RSPD2025R811), King Saud University, Riyadh, Saudi Arabia.

Author contributions: Neha Rana: writing – original draft; Neha Rana, Ankush M. Raut, Rudradev: resources and writing – review and editing; Ghadeer M. Albadrani, Muath Q. Al-Ghadi: methodology; Amany A. Sayed, Mohamed M. Abdel-Daim: methodology; Amany A. Sayed, Mohamed M. Abdel-Daim: formal analysis, writing – review and editing; A. Najitha Banu, Amine Assouguem: project administration, and writing – review and editing. All authors have read and agreed to the published version of the manuscript.

Conflicts of interest: The authors state no conflict of interest.

Data availability statement: All data generated or analyzed during this study are included in this published article.

References

[1] Becker J, Manske C, Randl S. Green chemistry and sustainability metrics in the pharmaceutical manufacturing sector. Curr Opin Green Sustain Chem. 2022;33:100562.

[2] Makarov VV, Love AJ, Sinitsyna OV, Makarova SS, Yaminsky IV, Taliansky ME, et al. "Green" nanotechnologies: synthesis of metal nanoparticles using plants. Acta Naturae (англоязычная версия). 2014;6(1 (20)):35–44.

[3] Cheng X, Huang J, Li H, Zhao D, Liu Z, Zhu L, et al. Quercetin: A promising therapy for diabetic encephalopathy through inhibition of hippocampal ferroptosis. Phytomedicine. 2024;126:154887.

[4] Naseer M, Aslam U, Khalid B, Chen B. Green route to synthesize Zinc Oxide Nanoparticles using leaf extracts of Cassia fistula and Melia azadarach and their antibacterial potential. Sci Rep. 2020;10(1):1–10, https://www.nature.com/articles/s41598-020-65949-3.

[5] Rauf MA, Oves M, Rehman FU, Khan AR, Husain N. Bougainvillea flower extract mediated zinc oxide's nanomaterials for antimicrobial and anticancer activity. Biomed Pharmacother. 2019;116:108983.

[6] Hameed H, Waheed A, Sharif MS, Saleem M, Afreen A, Tariq M, et al. Green synthesis of zinc oxide (ZnO) nanoparticles from green algae and their assessment in various biological applications. Micromachines (Basel). 2023;14(5):928. doi: 10.3390/mi14050928.

[7] Rana N, Singh SK, Banu NA, Hjazi A, Vamanu E, Singh MP. The ethnopharmacological properties of green-engineered metallic nanoparticles against metabolic disorders. Medicina. 2023;59(6):1022, https://www.mdpi.com/1648-9144/59/6/1022/htm.

[8] Najitha Banu A, Kudesia N, Rana N, Sadaf D, Raut AM. Antiparasitic activity of nanomaterials. Nanomaterials for sustainable development: Opportunities and future perspectives. Singapore: Springer; 2023. p. 173–205.

[9] Sarkar R, Rana N, Salaria B, Banu AN. Green ZnO nanoparticles: Potential for control of pests, mosquito diseases and antimicrobial agents. J Entomol Res. 2023;47:1011–5.

[10] El Golli A, Contreras S, Dridi C. Bio-synthesized ZnO nanoparticles and sunlight-driven photocatalysis for environmentally-friendly and sustainable route of synthetic petroleum refinery wastewater treatment. Sci Rep. 2023;13(1):1–14, https://www.nature.com/articles/s41598-023-47554-2.

[11] Akhtar MJ, Ahamed M, Kumar S, Khan MAM, Ahmad J, Alrokayan SA. Zinc oxide nanoparticles selectively induce apoptosis in human cancer cells through reactive oxygen species. Int J Nanomed. 2012;7:845–57.

[12] Moezzi A, McDonagh AM, Cortie MB. Zinc oxide particles: Synthesis, properties and applications. Chem Eng J. 2012;185:1–22.

[13] Kolodziejczak-Radzimska A, Jesionowski T. Zinc oxide – from synthesis to application: a review. Materials. 2014;7(4):2833–81, https://www.mdpi.com/1996-1944/7/4/2833/htm.

[14] Smijs TG, Pavel S. Titanium dioxide and zinc oxide nanoparticles in sunscreens: Focus on their safety and effectiveness. Nanotechnol Sci Appl. 2011;4(1):95–112. doi: 10.2147/NSA.S19419.

[15] Nithya K, Kalyanasundharam S. Effect of chemically synthesis compared to biosynthesized ZnO nanoparticles using aqueous extract of C. halicacabum and their antibacterial activity. OpenNano. 2019;4:100024.

[16] Zeng G, Wu Z, Cao W, Wang Y, Deng X, Zhou Y. Identification of anti-nociceptive constituents from the pollen of Typha angustifolia L. using effect-directed fractionation. Nat Prod Res. 2020;34(7):1041–5, https://www.tandfonline.com/doi/abs/10.1080/14786419.2018.1539979.

[17] Li W, Liu X, Liu Z, Xing Q, Liu R, Wu Q, et al. The signaling pathways of selected traditional Chinese medicine prescriptions and their metabolites in the treatment of diabetic cardiomyopathy: a review. Front Pharmacol. 2024;15:1416403.

[18] Luo P, Feng X, Liu S, Jiang Y. Traditional uses, phytochemistry, pharmacology and toxicology of Ruta graveolens L.: A critical review and future perspectives. Drug Des Devel Ther. 2024;18:6459–85, https://pubmed.ncbi.nlm.nih.gov/39758226/.

[19] Teleszko M, Wojdyło A, Rudzinska M, Oszmianski J, Golis T. Analysis of lipophilic and hydrophilic bioactive compounds content in sea buckthorn (Hippophae rhamnoides L.) berries. J Agric Food Chem. 2015;63(16):4120–9.

[20] Nouioura G, Tourabi M, El Ghouizi A, Kara M, Assouguem A, Saleh A, et al. Optimization of a new antioxidant formulation using a simplex lattice mixture design of Apium graveolens L. Plants J. 2023;12:1–15.

[21] Criste A, Urcan AC, Bunea A, Furtuna FRP, Olah NK, Madden RH, et al. Phytochemical composition and biological activity of berries and leaves from Four Romanian Sea Buckthorn (Hippophae Rhamnoides L.) varieties. Molecules. 2020;25(5):1170, https://pmc.ncbi.nlm.nih.gov/articles/PMC7179145/.

[22] Assouguem A, Kara M, Ramzi A, Annemer S, Kowalczyk A, Ali EA, et al. Evaluation of the effect of four bioactive compounds in combination with chemical product against two spider mites Tetranychus urticae and Eutetranychus orientalis (Acari: Tetranychidae). Evidence-Based Complement Altern Med. 2022;2022:2004623.

[23] Guo R, Guo X, Li T, Fu X, Liu RH. Comparative assessment of phytochemical profiles, antioxidant and antiproliferative activities of Sea buckthorn (Hippophaë rhamnoides L.) berries. Food Chem. 2017;221:997–1003.

[24] Ciesarová Z, Murkovic M, Cejpek K, Kreps F, Tobolková B, Koplík R, et al. Why is sea buckthorn (Hippophae rhamnoides L.) so exceptional? A review. Food Res Int. 2020;133:109170.

[25] Rupa EJ, Kaliraj L, Abid S, Yang DC, Jung SK. Synthesis of a zinc oxide nanoflower photocatalyst from sea buckthorn fruit for degradation of industrial dyes in wastewater treatment. Nanomaterials. 2019;9(12):1692. doi: 10.3390/nano9121692.

[26] Rana N, Banu AN, Kumar B, Singh SK, Abdel-Razik NE, Jalal NA, et al. Phytofabrication, characterization of silver nanoparticles using Hippophae rhamnoides berries extract and their biological activities. Front Microbiol. 2024;15:1399937.

[27] Naiel B, Fawzy M, Halmy MWA, Mahmoud AED. Green synthesis of zinc oxide nanoparticles using Sea Lavender (Limonium pruinosum L. Chaz.) extract: characterization, evaluation of anti-skin cancer, antimicrobial and antioxidant potentials. Sci Rep. 2022;12(1):20370.

[28] Safawo T, Sandeep BV, Pola S, Tadesse A. Synthesis and characterization of zinc oxide nanoparticles using tuber extract of anchote (Coccinia abyssinica (Lam.) Cong.) for antimicrobial and antioxidant activity assessment. OpenNano. 2018;3:56–63. doi: 10.1016/j.onano.2018.08.001.

[29] Haiouani K, Hegazy S, Alsaeedi H, Bechelany M, Barhoum A. Green synthesis of hexagonal-like ZnO nanoparticles modified with phytochemicals of clove (Syzygium aromaticum) and Thymus capitatus Extracts: Enhanced antibacterial, antifungal, and antioxidant activities. Materials. 2024;17(17):4340.
[30] Kaur M, Singh K, Kumar V. Green synthesis of silver nanoparticles using Penicillium camemberti and its biological applications. Bionanoscience. 2024;1–15.
[31] Badmus JA, Adedosu TO, Fatoki JO, Adegbite VA, Adaramoye OA, Odunola OA. Lipid peroxidation inhibition and antiradical activities of some leaf fractions of Mangifera indica. Acta Pol Pharm. 2011;68(1):23–9.
[32] Majeed S, Danish M, Zakariya NA, Hashim R, Ansari MT, Alkahtani S, et al. *In vitro* evaluation of antibacterial, antioxidant, and antidiabetic activities and glucose uptake through 2-NBDG by Hep-2 liver cancer cells treated with green synthesized silver nanoparticles. Oxid Med Cell Longev. 2022;2022(1):1646687.
[33] Balouiri M, Sadiki M, Ibnsouda SK. Methods for *in vitro* evaluating antimicrobial activity: A review. J Pharm Anal. 2016;6(2):71–9.
[34] Sohn EK, Johari SA, Kim TG, Kim JK, Kim E, Lee JH, et al. Aquatic toxicity comparison of silver nanoparticles and silver nanowires. Biomed Res Int. 2015;2015(1):893049.
[35] Thirumal S, Senthilkumar SR, Sivakumar T. Green tea (Camellia sinensis) mediated synthesis of zinc oxide (ZnO) nanoparticles and studies on their antimicrobial activities. Int J Pharm Pharm Sci. 2014;6(6):461–5.
[36] Krilov D, Balarin M, Kosović M, Gamulin O, Brnjas-Kraljević J. FT-IR spectroscopy of lipoproteins – A comparative study. Spectrochim Acta A Mol Biomol Spectrosc. 2009;73(4):701–6.
[37] Albarakaty FM, Alzaban MI, Alharbi NK, Bagrwan FS, Abd El-Aziz ARM, Mahmoud MA. Zinc oxide nanoparticles, biosynthesis, characterization and their potent photocatalytic degradation, and antioxidant activities. J King Saud Univ Sci. 2023;35(1):102434.
[38] Stan M, Popa A, Toloman D, Silipas TD, Vodnar DC. Antibacterial and antioxidant activities of ZnO nanoparticles synthesized using extracts of Allium sativum, Rosmarinus officinalis and Ocimum basilicum. Acta Metallurgica Sinica (English Letters). 2016;29(3):228–36, https://link.springer.com/article/10.1007/s40195-016-0380-7.
[39] Brishti RS, Ahsan Habib M, Ara MH, Rezaul Karim KM, Khairul Islam M, Naime J, et al. Green synthesis of ZnO NPs using aqueous extract of Epipremnum aureum leave: Photocatalytic degradation of Congo red. Results Chem. 2024;7:101441, https://www.sciencedirect.com/science/article/pii/S2211715624001371#b0230.
[40] Parvathalu K, Chinmayee S, Preethi B, Swetha A, Maruthi G, Pritam M, et al. Green synthesis of silver nanoparticles using Argyreia nervosa leaf extract and their antimicrobial activity. Plasmonics. 2023;18(3):1075–81, https://link.springer.com/article/10.1007/s11468-023-01835-8.
[41] Wu F, Harper BJ, Harper SL. Comparative dissolution, uptake, and toxicity of zinc oxide particles in individual aquatic species and mixed populations. Env Toxicol Chem. 2019;38(3):591. Available from:/pmc/articles/PMC6446720/.
[42] Lopes S, Ribeiro F, Wojnarowicz J, Lojkowski W, Jurkschat K, Crossley A, et al. Zinc oxide nanoparticles toxicity to Daphnia magna: size-dependent effects and dissolution. Env Toxicol Chem. 2014;33(1):190–8, https://onlinelibrary.wiley.com/doi/full/10.1002/etc.2413.
[43] Santos-Rasera JR, Monteiro RTR, de Carvalho HWP. Investigation of acute toxicity, accumulation, and depuration of ZnO nanoparticles in Daphnia magna. Sci Total Environ. 2022;821:153307.
[44] Bacchetta R, Santo N, Marelli M, Nosengo G, Tremolada P. Chronic toxicity effects of ZnSO4 and ZnO nanoparticles in Daphnia magna. Env Res. 2017;152:128–40.
[45] Bharadwaj KK, Rabha B, Pati S, Choudhury BK, Sarkar T, Gogoi SK, et al. Green Synthesis of Silver Nanoparticles Using Diospyros malabarica Fruit Extract and Assessments of Their Antimicrobial, Anticancer and Catalytic Reduction of 4-Nitrophenol (4-NP). Nanomaterials. 2021;11(8):1999, https://www.mdpi.com/2079-4991/11/8/1999/htm.
[46] Elemike EE, Onwudiwe DC, Ogeleka DF, Obasi EC. Biomediated cellulose-Ag-ZnO nanocomposites and their ecotoxicological assessment using onion bulb plant. J Clust Sci. 2021;32(3):651–6, https://link.springer.com/article/10.1007/s10876-020-01826-3.
[47] Shabir S, Sehgal A, Dutta J, Devgon I, Singh SK, Alsanie WF, et al. Therapeutic potential of green-engineered ZnO nanoparticles on rotenone-exposed D. melanogaster (Oregon R+): Unveiling ameliorated biochemical, cellular, and behavioral parameters. Antioxidants. 2023;12(9):1679.
[48] Engida AM, Faika S, Nguyen-Thi BT, Ju YH. Analysis of major antioxidants from extracts of Myrmecodia pendans by UV/visible spectrophotometer, liquid chromatography/tandem mass spectrometry, and high-performance liquid chromatography/UV techniques. J Food Drug Anal. 2014;23(2):303, https://pmc.ncbi.nlm.nih.gov/articles/PMC9351773/.
[49] Khan MR, Hoque SM, Hossain KFB, Siddique MAB, Uddin MK, Rahman MM. Green synthesis of silver nanoparticles using Ipomoea aquatica leaf extract and its cytotoxicity and antibacterial activity assay. Green Chem Lett Rev. 2020;13(4):39–51.
[50] Flemban TH. Synthesis of ZnO nanoparticles using varying pulsed laser ablation energies in liquid; 2022, https://www.researchsquare.com/article/rs-2043982/v1.
[51] Siripireddy B, Mandal BK. Facile green synthesis of zinc oxide nanoparticles by Eucalyptus globulus and their photocatalytic and antioxidant activity. Adv Powder Technol. 2017;28(3):785–97.
[52] Reed TT. Lipid peroxidation and neurodegenerative disease. Free Radic Biol Med. 2011;51(7):1302–19.
[53] Abhinaya SR, Padmini R. Biofabrication of zinc oxide nanoparticles using pterocarpus marsupium and its biomedical applications. Asian J Pharm Clin Res. 2019;12(1):245–9. doi: 10.22159/ajpcr.2019.v12i1.28682.
[54] Zhelev I, Petkova Z, Kostova I, Damyanova S, Stoyanova A, Dimitrova-Dyulgerova I, et al. Chemical composition and antimicrobial activity of essential oil of fruits from Vitex agnus-castus L., growing in two regions in Bulgaria. Plants. 2022;11:896. doi: 10.3390/plants11070896.
[55] Valgimigli L. Lipid peroxidation and antioxidant protection. Biomolecules. 2023;13(9). Available from:/pmc/articles/PMC10526874/.
[56] Kambale EK, Katemo FM, Quetin-Leclercq J, Memvanga PB, Beloqui A. “Green”-synthesized zinc oxide nanoparticles and plant extracts: A comparison between synthesis processes and antihyperglycemic activity. Int J Pharm. 2023;635:122715.
[57] Siddiqui SA, Rashid MMO, Uddin MG, Robel FN, Hossain MS, Haque MA, et al. Biological efficacy of zinc oxide nanoparticles against diabetes: a preliminary study conducted in mice. Biosci Rep. 2020;40(4):20193972. Available from:/pmc/articles/PMC7138905/.
[58] Zhao Z, Cao Y, Xu R, Fang J, Zhang Y, Xu X, et al. Nanoparticles (NPs)-mediated targeted regulation of redox homeostasis for effective cancer therapy. Smart Mater Med. 2024;5(2):291–320.
[59] Shoaib A, Shahid S, Mansoor S, Javed M, Iqbal S, Mahmood S, et al. Tailoring of an anti-diabetic drug empagliflozin onto zinc oxide

nanoparticles: characterization and *in vitro* evaluation of anti-hyperglycemic potential. Sci Rep. 2024;14(1):1–14, https://www.nature.com/articles/s41598-024-52523-4.

[60] Xiang YX, Xu Z, Xiao R, Yao YL, Tang XJ, Fu LJ, et al. Interacting and joint effects of assisted reproductive technology and gestational diabetes mellitus on preterm birth and the mediating role of gestational diabetes mellitus: a cohort study using a propensity score. J Assist Reprod Genet. 2025;42(2):489–98, https://link.springer.com/article/10.1007/s10815-024-03342-z.

[61] Slavin YN, Asnis J, Häfeli UO, Bach H. Metal nanoparticles: understanding the mechanisms behind antibacterial activity. J Nanobiotechnology. 2017;15(1):65.

[62] Huq MA, Apu MAI, Ashrafudoulla M, Rahman MM, Parvez MAK, Balusamy SR, et al. Bioactive ZnO nanoparticles: Biosynthesis, characterization and potential antimicrobial applications. Pharmaceutics. 2023;15(11):2634.

[63] Yin IX, Zhang J, Zhao IS, Mei ML, Li Q, Chu CH. The antibacterial mechanism of silver nanoparticles and its application in dentistry. Int J Nanomed. 2020;15:2555–62, https://www.tandfonline.com/action/journalInformation?journalCode=dijn20.

[64] Lal H, Misra V, Viswanathan PN, Krishna Murti CR. The water flea (Daphnia magna) as a sensitive indicator for the assessment of toxicity of synthetic detergents. Ecotoxicol Env Saf. 1984;8(5):447–50, https://pubmed.ncbi.nlm.nih.gov/6489240/.

[65] Ebert D. Daphnia as a versatile model system in ecology and evolution. EvoDevo. 2022;13(1):1–13, https://evodevojournal.biomedcentral.com/articles/10.1186/s13227-022-00199-0.